UMYU Scientifica, Vol. 4 NO. 4, December 2025, Pp 295 – 300
https://doi.org/10.56919/usci.2544.026
ISSN: 2955 – 1145 (print); 2955 – 1153 (online)
A periodical of the Faculty of Natural and Applied Sciences, UMYU, Katsina

ORIGINAL RESEARCH ARTICLE

Estimation of the Production Cross Sections of Medical ^{61}Cu Radioisotope Using EXIFON Code

Emmanuel J. Adoyi[1], Olumide O. Ige[1], Sunday A. Jonah[2], Abel B. Olorunsola[3] and Abraham F. Olalowo[4]

[1]Department of Physics, Nigerian Defence Academy, Kaduna, Kaduna State, Nigeria
[2]Centre for Energy Research and Training, Ahmadu Bello University, Zaria, Nigeria
[3]Department of Physics, Faculty of Science, University of Abuja, FCT Abuja, Nigeria
[4]School of Preliminary Studies, Faculty of Science, Nile University of Nigeria, Abuja, Nigeria

ABSTRACT

PET relies on short-lived radionuclides, such as ^{18}F-FDG, but their limited half-lives limit clinical applications. Copper-61 (^{61}Cu), a promising non-standard positron emitter with a $T_{1/2}$ of 3.33 hours, offers advantages for imaging slower biological processes. This study evaluates the cross-sections for ^{61}Cu production on enriched nickel targets: ^{61}Ni(p,n)^{61}Cu and ^{62}Ni(p,2n)^{61}Cu, using EXIFON 2.0 code. The calculations incorporated shell structure effects and compared the results with those of other studies. For ^{61}Ni(p,n)^{61}Cu, the cross-section, showing reasonable comparison of 3.3% with measured data up to 11 MeV but diverging at higher energies, likely due to pre-equilibrium contributions. Comparative analysis revealed ^{61}Ni(p,n)^{61}Cu as the optimal route for ^{61}Cu production, yielding higher cross sections at lower energies, thereby reducing costs and complexity. This work underscores the viability of ^{61}Ni(p,n)^{61}Cu for cyclotron-based ^{61}Cu production and supports its potential for PET imaging.

ARTICLE HISTORY

Received June 29, 2025
Accepted December 16, 2025
Published December 30, 2025

KEYWORDS

Copper-61, Shell structure effect, EXIFON 2.0 Code, Positron emission Tomography

INTRODUCTION

Pharmaceuticals that are always positron emitters are used in Positron Emission Tomography (PET). For example, ^{18}F-FDG (fluorodeoxyglucose) is used as a radiopharmaceutical in glucose metabolism. In the context of staging and therapeutic monitoring in cancer patients, ^{18}F-FDG is primarily used for whole-body imaging. It is used in pre-clinical studies (cancer research), mapping normal human brain and heart function, and detecting pairs of gamma rays indirectly released by a positron-emitting radionuclide (tracer) (Aslam and Qaim, 2014). The short half-life of many of the radionuclides used in PET limits its widespread applications worldwide. This is because producing the short-lived radionuclide for PET scanning requires a costly cyclotron co-located with the PET facility.

Since any organic carrier for the radioisotope is destroyed by cyclotron bombardment during preparation, the organic radioisotope cannot be synthesized first and then prepared within it. These short-lived positron emitters of light elements are [^{11}C ($T_{1/2}$=20min), ^{13}N ($T_{1/2}$=10min), ^{15}O ($T_{1/2}$=2min), and ^{18}F ($T_{1/2}$=110min)] and are generally found in organic compounds. This restriction primarily limits clinical PET to tracers tagged with fluorine-18, which has a half-life of 110 minutes and can be manufactured at a decent distance before use, unlike other short-lived positron emitters, which decay quickly due to their short half-lives.

More focus is being placed on the creation of non-standard positron emitters, or those with longer lifetimes. These include copper isotopes with a variety of medicinal applications, such as ^{60}Cu ($T_{1/2}$ = 23.7min), ^{62}Cu ($T_{1/2}$ = 9.7min), ^{64}Cu ($T_{1/2}$ = 12.7h), and ^{67}Cu ($T_{1/2}$ = 61.8h) (Blower et al., 1996: Anderson et al., 2003: Rowshanfarazad 2006). ^{61}Cu ($T_{1/2}$= 3.33h) is another copper radionuclide that could be useful in nuclear medicine (Szelecsenyi et al., 1993). It decays predominantly by positron emission (Iβ+ = 62%; Eβ+ = 1.159Mev; EC = 38%) with notable ϒ-rays at 283KeV (12%) and 656KeV (10.8%) as companion particles.

^{61}Cu is considered superior to ^{64}Cu for imaging due to its shorter half-life and a more pronounced positron decay branching ratio, which can result in higher image quality. Its rapid optimal uptake within 1-4 hours makes its brief half-life advantageous (McCarthy et al., 1999; Cutler et al., 1999). Moreover, ^{61}Cu exhibits a similar radiation dosage

Correspondence: Emmanuel Joseph Adoyi. Department of Physics, Faculty of Sciences, Nigerian Defence Academy, Kaduna, Nigeria. ✉ jeadoyi@nda.edu.ng.

How to cite: Adoyi, E. J., Ige, O. O., Jonah, S. A., Olorushola, A. B., & Olalowo, A. F. (2025). Estimation of the Production Cross Sections of Medical ^{61}Cu Radioisotope Using EXIFON Code. *UMYU Scientifica*, 4(4), 295 – 300. https://doi.org/10.56919/usci.2544.026

to ^{18}FDG (William et al., 2005) and a longer half-life than ^{60}Cu and ^{62}Cu, making it suitable for prolonged imaging of slow kinetic processes (Szelecsenyi et al., 2005; Rowshanfarzad et al., 2006). This study investigates nickel targets for ^{61}Cu production, noting that 61Cu can also be produced on a medical cyclotron from zinc, nickel, or cobalt using proton, deuteron, or alpha particles.

A review of archived cross-sections in the EXFOR database frequently reveals significant discrepancies between different observations, even within the same energy region. While pinpointing the precise causes of these inconsistencies is challenging, they are commonly attributed to uncertainties in factors such as monitor cross-sections, calibration sources, and detector efficiency. To address this, a comprehensive data evaluation process is crucial for generating a reliable, accepted dataset for a specific reaction. Accurate nuclear reaction cross-sections are fundamental for optimizing radionuclide production, evaluating various nuclear models, and deepening understanding of nuclear reaction mechanisms.

The experimental determination of cross-sections for short-lived copper radioisotopes is inherently difficult. Consequently, there has been an increasing focus on production cross-sections calculated using nuclear codes (Uncu and Ozdogan, 2023). However, theoretical model conclusions often lack strong agreement with experimental data. Theoretical calculations are typically adjusted to experimental data using a range of nuclear approximations, including level density, gamma-strength functions, and optical potential models. This reliance on multiple models for calculations leads to variability and uncertainty in cross-section values. Despite the application of various codes and sophisticated statistical analyses to mitigate this issue, the desired outcomes are not consistently achieved (Uncu and Ozdogan, 2023). This investigation will specifically examine the copper-61 production routes via (p,n) and (p,2n) reactions, with EXIFON 2.0 employed for a critical evaluation of their excitation functions.

MATERIAL AND METHODS

H. Kalka developed the EXIFON analytical model from a purely statistical multistep reaction framework. It provides a distinct description of emission spectra, angular distributions, and activation cross sections, encompassing equilibrium, pre-equilibrium, and direct theory processes (both collective and non-collective). The model is grounded in extensive research on Green's function formalism and random matrix physics. The shift from simpler single-step direct models and the basic compound nucleus model to statistical multistep theories was primarily influenced by three significant concepts: the treatment of the chaotic nuclear Hamiltonian as a random matrix (D. Agassi et al., 1975), the differentiation between bound and unbound state configurations (Feshbach et al., 1980), and the classification of nuclear states based on their complexity or exciton numbers (Griffin, 1967).

The EXIFON code computation in this study was based on the Optical Model (OM) formalism for the Statistical Multistep Compound (SMC), Statistical Multistep Direct (SMD), and Multi-Particle Emission (MPE) processes. This technique will forecast angular distributions, activation cross sections, and emission spectra, including equilibrium and pre-equilibrium events. The model permits the induction of reactions using neutrons, protons, alphas, and photons in the outgoing channels, but it prohibits the employment of gamma and heavy charged particles as incident particles (Kalka 1991). For this study, the ^{61}Ni and ^{62}Ni nickel isotopes were examined using the EXIFON method.

To comprehensively assess all conceivable scenarios regarding the influence of shell structure on interactions, and drawing upon data from the computational code, the reactions (p, n) and (p, 2n) were investigated from 1 – 20 MeV.

During the execution of each computational analysis, the input and output directories are initially delineated, followed by the specification of the target nuclei as ^{61}Ni and ^{62}Ni. The incident particle pertinent to this investigation is the proton, which is subsequently selected, while the Excitation Function is designated as the overarching option for the calculations. In the following step, the number of incident energy levels is defined as 20 MeV, thereby indicating the maximum incident energy considered for the analysis, which is succeeded by the specification of the initial incident energy set at 1 MeV, denoting the minimum energy for which the cross-section is to be computed; thereafter, the incident energy increment is established at 1 MeV to delineate the energy scale for the cross-section calculations. Moreover, in the modification section, this study exclusively examines the effects of shell structure, applying its two shell-correction options to each reaction channel. The OUTEXI file for each current computation is meticulously saved either in the working directory or in an alternative location.

The phenomenon of shell structure is manifested in Statistical Multistep Compound (SMC) processes, wherein the single-particle state density g, as delineated in equation (1) (Ignatius et al., 1975), is augmented by the resulting outcomes.

$$g = (1 + \frac{\delta W}{E_X}\,[\,1 - exp\,(-\gamma E_X)]) \qquad (1)$$

The shell correction energy is represented by γ = 0.05 MeV^{-1} and the excitation energy of the residual systems is indicated by the amount E_X= E or U, respectively. Both shell corrections (δW = 0) and (δW ≠ 0) were used in the computations. Cross-sectional findings were obtained by conducting the methods WITH and WITHOUT shell correction multiple times. This forecasts the activation of neutrons, protons, alpha particles, and photons as well as their angular distributions, emission spectra, and cross sections. It is also possible to arrange the EXIFON output into ENDF/B-6 format.

RESULTS AND DISCUSSION

Evaluation of the production data of ^{61}Cu

^{61}Ni(p,n)^{61}Cu

Several writers have examined the proton-induced reaction on ^{61}Ni as a potential method for producing ^{61}Cu, while accounting for various model parameters. According to Aslam and Qaim (2014), this reaction is an effective way to produce ^{61}Cu, even though it requires the use of costly enriched ^{61}Ni as the target material. Several tests were conducted using enriched ^{61}Ni target, with Szelecsenyi et al. (1993) performing the most comprehensive measurement. None of the targets, nevertheless, was completely enriched. The remaining measurements, as described by Blaser et al. (1951), were carried out using ^{nat}Ni target foils.

The ^{61}Ni(p,n)^{61}Cu reaction's excitation curve is shown in Figure 1, and equation (2) (wong, 1998) indicates that the reaction's threshold energy is between 3 and 4 MeV.

$$T_p \geq -Q\left(\frac{M_T+m_p}{M_T}\right) \quad (2)$$

This compares well with the calculated threshold energy for reaction obtained as 3.07MeV using the well-known formalism and using Q from Blaser *et al.* (1951).

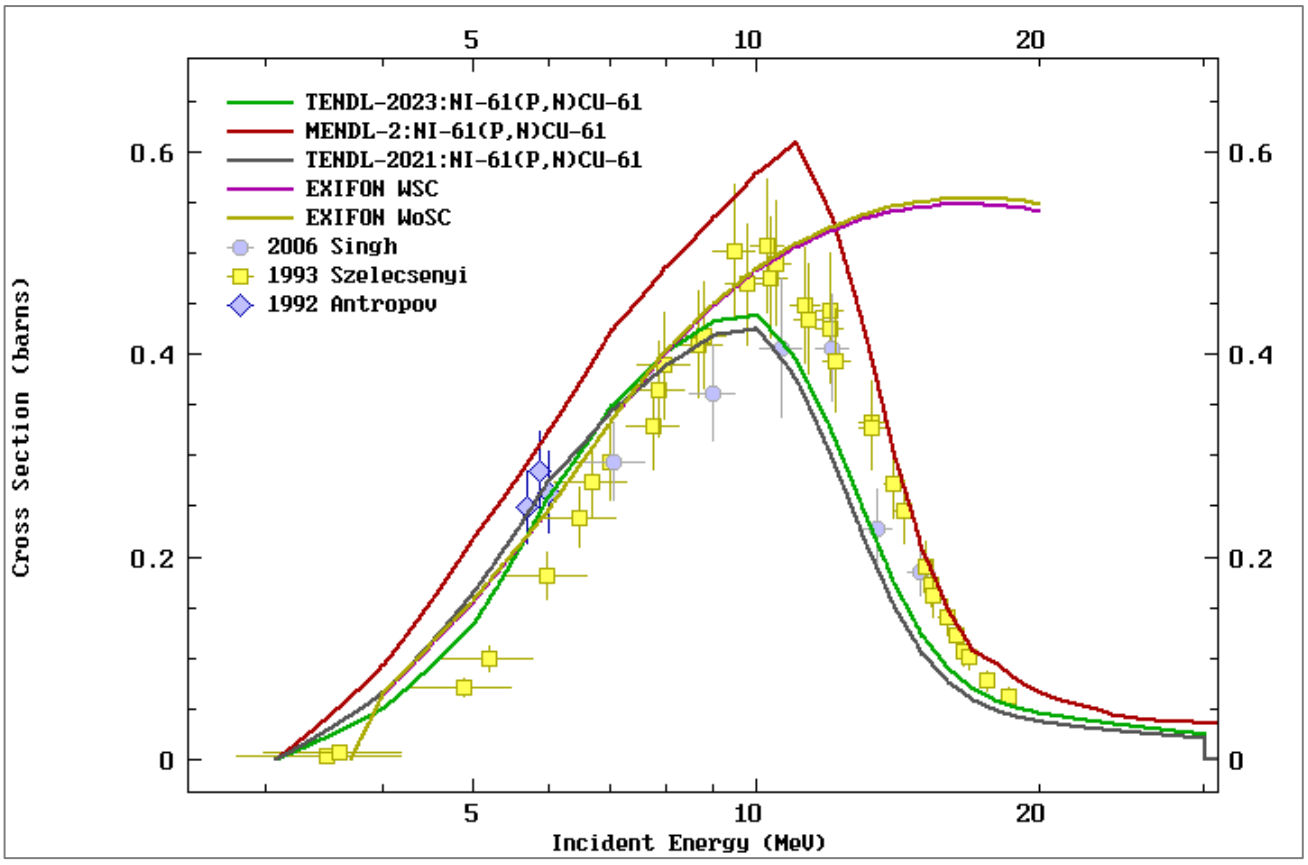

Figure 1: Plot of ^{61}Ni(p,n) ^{61}Cu reaction.

The calculated cross sections with shell correction (WSC) and without shell correction (WoSC) appear to agree fairly well up to 20 MeV, with percentage differences mostly less than 1%. The two values compare very closely and are consistent throughout the entire energy range. Furthermore, both show a 3.3% difference compared with the predicted result by TENDL (2023) and the measured data from Szelecsenyi et al. (1993) up to about 11 MeV. Our work differs significantly from the TENDL (2023) evaluation, which has a lower cross-section at 11 MeV.

The deviation of our calculation and TENDL (2023) may be attributed to the pre-equilibrium model used at higher energy. The direct energy dependence of the cross section from the threshold energy of 4 MeV to 11 MeV for cross sections with wsc, wosc, ENDF, and measurements appears consistent with known compound-nucleus theory. (Borh, 1936) Excitation function curves, whose cross section rises sharply beyond the reaction threshold and falls as a result of competitive reaction and the increase of the quantum mechanical pre-equilibrium contribution with proton energy, are a common feature of compound nucleus production (Feshbach et al. 1980)

Our calculations, when compared with other studies (Figure 1), show a significant deviation, suggesting the need for the optical model in the calculation of proton-induced reactions on light-size nuclei, which start at about 5 MeV and become significantly important at about 11 MeV. Thus, a pre-equilibrium description of the (p,n)

reaction channel of ^{61}Ni, as done in EXIFON require accounting for the optical model contribution. This was achieved by calculating Aslam using the EMPIRE code, which compared well with the measured data from Szelecsenyi.

The calculated data of Aslam and Qaim (2014) using the EMPIRE and TALYS codes accounted for the optical model, compound-nucleus, and pre-equilibrium models comprehensively up to 20 MeV.

^{62}Ni(p,2n)^{61}Cu

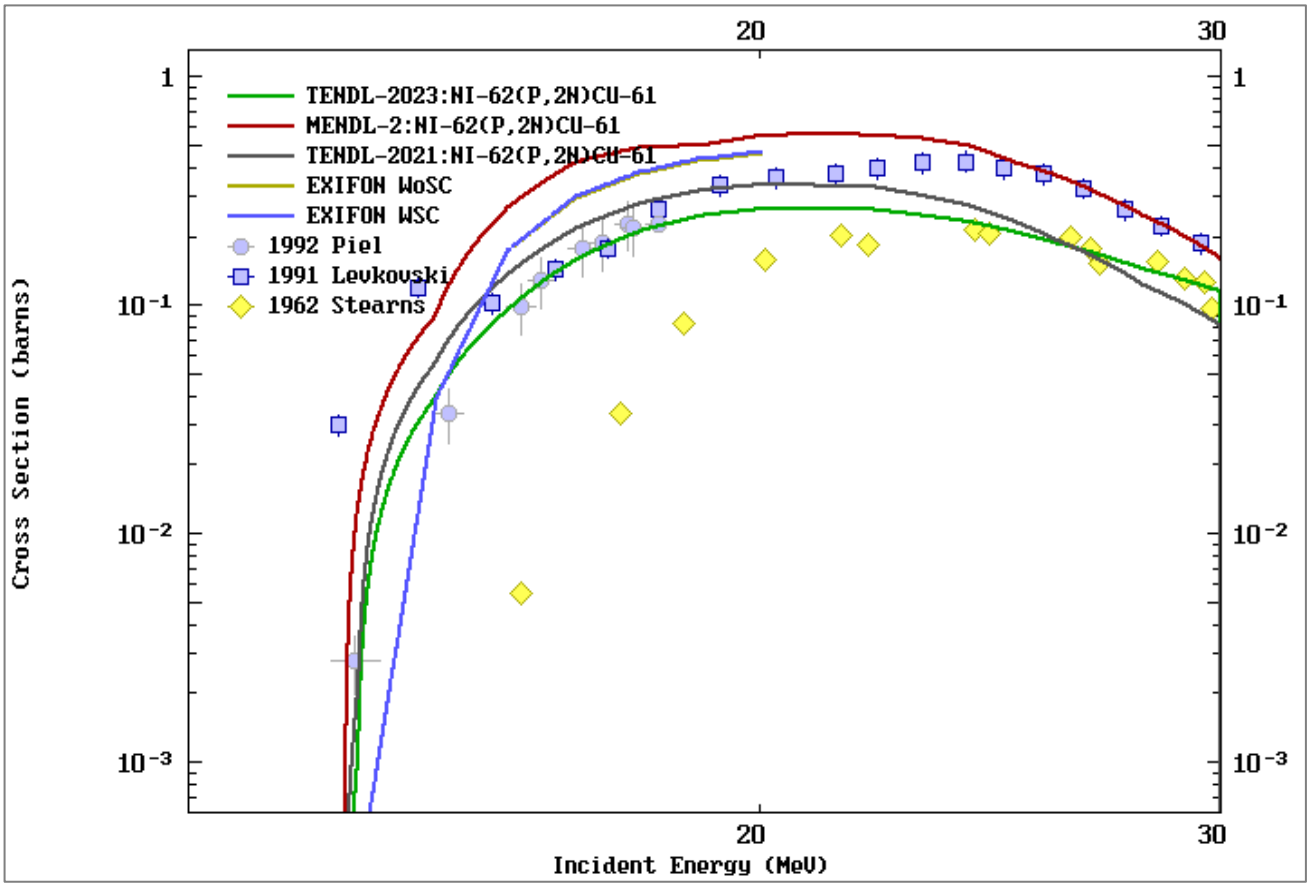

Figure 2: Plot of ^{62}Ni(p,2n)^{61}Cu reaction

The ^{62}Ni(p,2n)^{61}Cu reaction's excitation function is shown in Figure 2. The computation shows that the reaction cross section's threshold energy lies between 14 and 15 MeV. The threshold energy for the reaction, determined to be 13.87 MeV using a Q-value of -13.6 from Piel et al. (1992), compares favourably with this value. The (p,2n) reaction cross section for ^{62}Ni at 15 MeV is 37.5 mb for calculations with a shell structure correction and 37.1 mb for calculations without a correction up to 20 MeV; the two computations compare closely, with a percentage difference of 1-3%. This indicates strong consistency between the two sets of cross-section values.

Figure 2 plots the results of the ^{62}Ni(p,2n)^{61}Cu excitation calculations along with the experimental data file that was obtained from the EXFOR data library and the evaluated data file that was obtained, ENDF (ENDF/B. VII.1. TENDL, MENDL). The graph shows that the calculations match well with both the ENDF data file (ENDF/B. VII.1. TENDL, MENDL) and the experimental data (EXFOR). Nevertheless, there are differences between the data collected for this study and the data retrieved from the EXFOR trial, as well as the analyzed data from MENDL and TENDL, due to differences in the models of the codes.

Comparative Analysis of (P, N) and (P, 2N) Reactions

In comparing the (p,n) reaction channel of ^{61}Ni both for wsc and wosc is more probable as it can be observed from Table 1. at 4 MeV, the shell effect without correction produced a cross section of 63mb as compare to 60.9mb for wsc at the same energy level and the reaction channel (p,n) for ^{62}Ni is more probable for with shell effect correction from the Table as at 6 Mev it generate a cross section of 319.9mb which is higher than without shell effect correction with cross section of 316.8mb at the same energy level. However, this reaction channel for ^{62}Ni is not preferred, as we are interested in producing ^{61}Cu rather than ^{62}Cu.

In comparing the (p,2n) reaction channel of ^{62}Ni for wsc and wosc, the shell effect with correction is more probable, as shown in Table 1. At 15 MeV, the reaction channel (p,2n) with shell effect correction generate a cross section of 37.5mb while without shell effect correction at the same energy level it is 37.1mb which means to produce ^{61}Cu from calculation using the EXIFON 2.0 computational code with shell structure being the only adjustable parameter, with production channel (p,n)

without shell effect correction is more probable while with production channel (p,2n) with shell effect correction is more probable. Also, the more probable reaction channel for ^{61}Cu production is ^{61}Ni(p,n)^{61}Cu, as it generates a cross section at a low proton energy of 4 MeV, unlike the ^{62}Ni(p,2n)^{61}Cu channel, which requires an energy of 15 MeV to generate an output. At 15 MeV, the production channel ^{61}Ni(p,n)^{61}Cu can have a cross section of 551.7, which is larger than that of the production channel ^{62}Ni(p,2n)^{61}Cu, which is 37.5 mb at the same proton energy. From this analysis, it can be deduced that the reaction channel ^{61}Ni(p,n)^{61}Cu is a more probable channel for the production of ^{61}Cu for medical applications in PET.

Table 1: Calculated cross-section data of (p,n) and (p,2n)

Energy (MeV)	Wsc (p,n) mb		Wosc (p,n) mb		Wsc (p,2n) mb		wosc(p,2n) mb	
	^{61}Ni	^{62}Ni	^{61}Ni	^{62}Ni	^{61}Ni	^{62}Ni	^{61}Ni	^{62}Ni
4	60.9	0.0	63.0	0.0	0.0	0.0	0.0	0.0
5	156.2	0.0	156.7	0.0	0.0	0.0	0.0	0.0
6	244.4	319.9	244.9	316.8	0.0	0.0	0.0	0.0
7	333.3	445.6	334.2	441.8	0.0	0.0	0.0	0.0
8	402,2	543.6	403.7	538.4	0.0	0.0	0.0	0.0
9	449.6	612.9	451.8	606.1	0.0	0.0	0.0	0.0
10	482.8	662.1	485.8	653.4	0.0	0.0	0.0	0.0
11	506.3	697.4	509.8	686.8	0.0	0.0	0.0	0.0
12	522.7	722.6	526.8	710.0	0.0	0.0	0.0	0.0
13	534.4	740.8	539.0	726.3	0.0	0.0	0.0	0.0
14	541.8	752.6	546.9	736.3	0.0	0.0	0.0	0.0
15	546.3	759.7	551.7	741.8	0.0	37.5	0.0	37.1
16	548.3	763.3	554.2	743.6	13.0	176.7	11.5	174.0
17	548.8	763.7	554.8	742.6	71.4	301.8	64.5	296.1
18	547.7	761.8	554.0	739.2	140.5	389.4	129.1	380.5
19	545.6	757.9	552.0	734.2	198.6	442.4	184.4	431.0
20	542.5	752.4	549.1	727.6	230.3	470.8	215.3	457.5

CONCLUSION

The EXIFON 2.0 Code was used to estimate the cross-section of the ^{61}Ni(p,n)^{61}Cu and ^{62}Ni(p,2n)^{61}Cu reactions from threshold to 20 MeV. Reaction cross-section calculations were compared with the evaluated data from ENDF data files (ENDF/B-VII.1, MENDL, TENDL) and experimental data from EXFOR. The results showed a considerable deviation for ^{62}Ni(p,n)^{61}Cu at a projectile energy of 11 MeV, but they are 3.3% compared with measurements and are in excellent agreement with the ^{62}Ni(p,2n)^{61}Cu reaction. To optimize different approaches for generating ^{61}Cu at a cyclotron for PET use, the study recommends the ^{61}Ni(p,n)^{61}Cu reaction channel.

REFERENCE

Anderson, C. J., Green, M. A., & Fujibayashi, Y. (2003). Chemistry of copper radionuclides and radiopharmaceutical products. In M. J. Welch & C. S. Redvanly (Eds.), *Handbook of radiopharmaceuticals: Radiochemistry and applications* (pp. 400–422). Wiley. [Crossref]

Aslam, M. N., & Qaim, S. M. (2014). Nuclear model analysis of excitation functions of proton, deuteron and α-particle induced reactions on nickel isotopes for production of the medically interesting copper-61. *Applied Radiation and Isotopes, 89*, 65–73. [Crossref]

Blaser, J. P., Boehm, F., Marmier, P., & Preiswerk, P. (1951). Excitation functions of proton-induced nuclear reactions. *Helvetica Physica Acta*, 24, 441–460.

Blower, P. J., Lowes, J. S., & Zweit, J. (1996). Copper radionuclides and radiopharmaceuticals in nuclear medicine. *Nuclear Medicine and Biology, 23*(8), 957–980. [Crossref]

Bohr, N. (1936). Neutron capture and nuclear constitution. *Nature, 137*(3461), 344–348. [Crossref]

Cutler, C. S., Lewis, J. S., & Anderson, C. J. (1999). Utilization of metabolic, transport and receptor-mediated processes to deliver agents for cancer diagnosis. *Advanced Drug Delivery Reviews, 37*(1–3), 189–211. [Crossref]

Exfor N. R. D. (2018). *EXFOR* [Database]. International Network of Nuclear Reaction Data Centres. [Link]

Feshbach, H., Kerman, A. K., & Koonin, S. E. (1980). The statistical theory of multi-step compound and direct reactions. *Annals of Physics, 125*(2), 429–476. [Crossref]

Griffin, J. J. (1967). Statistical model of intermediate structure. *Physical Review Letters*, 17(9), 478–481. [Crossref]

Ignatyuk, A. V., Smirenkin, G. N., & Tishin, A. S. (1975). Phenomenological description of energy dependence of the level density parameter. *Soviet Journal of Nuclear Physics, 21*(3), 255–257. (Original work published 1975) [Crossref]

Kalka, H. (1991). *EXIFON—A statistical multi-step reaction code*. Technische Universität Dresden.

Koning, A. J., Rochman, D., Sublet, J.-Ch., Dzysiuk, N., Fleming, M., & van der Marck, S. (2019).

TENDL: Complete nuclear data library for innovative nuclear science and technology. *Nuclear Data Sheets, 155*, 1–55. [Crossref]

McCarthy, D. W., Bass, L. A., Cutler, P. D., Shefer, R. E., Klinkow-stein, R. E., Herrero, P., Lewis, J. S., Cutler, C. S., Anderson, C. J., & Welch, M. J. (1999). High purity production and potential applications of copper-60 and copper-61. *Nuclear Medicine and Biology, 26*(4), 351–358. [Crossref]

Piel, H., Qaim, S. M., & Stöcklin, G. (1992). Excitation functions of (p, xn)-reactions on natNi and highly enriched 62Ni: Possibility of production of medically important radioisotope 62Cu at a small cyclotron. *Radiochimica Acta*, 57(1), 1–6. [Crossref]

Rowshanfarazad, P., Sabet, M., Jalilian, A. R., & Kamalidehghan, M. (2006). An overview of copper radionuclides and production of 61Cu by proton irradiation of natZn at a medical cyclotron. *Applied Radiation and Isotopes, 64*(12), 1563–1573. [Crossref]

Rowshanfarzad, P., Vinitsky, S. I., Bezak, E., & Boxenhorn, B. (2006). Monte Carlo investigation of quasi-elastic and non-elastic interactions for proton therapy and radionuclide production. *Nuclear Instruments and Methods in Physics Research Section B: Beam Interactions with Materials and Atoms*, 247(2), 365–375. [Crossref]

Szelecsenyi, F., Blessing, G., & Qaim, S. M. (1993). Excitation functions of proton induced nuclear reactions on enriched 61Ni and 64Ni: Possibility of production of no-carrier-added 61Cu and 64Cu at a small cyclotron. *Applied Radiation and Isotopes, 44*(3), 575–580. [Crossref]

Szelecsényi, F., Tarkanyi, F., Takács, S., & Ditroi, F. (2005). Investigation of production routes of 61Cu and 64Cu on enriched 60Ni and 64Ni targets. *Applied Radiation and Isotopes*, 62(1), 133–147. [Crossref]

TENDL Nuclear Data Library. (2023). *TENDL 2023: TALYS-based evaluated nuclear data library* [Data set]. [Link]

Uncu, Y. A., & Ozdogan, H. (2023). Estimations for the production cross sections of medical 61,64,67Cu radioisotopes by using Bayesian regularized artificial neural networks in (p,α) reactions. *Arabian Journal for Science and Engineering, 48*(6), 8173–8179. [Crossref]

Williams, H. A., Robinson, S., Julyan, P., Zweit, J., & Hastings, D. (2005). A comparison of PET imaging characteristics of various copper radioisotopes. *European Journal of Nuclear Medicine and Molecular Imaging, 32*(12), 1473–1480. [Crossref]

Wong, S. S. M. (1998). *Introductory nuclear physics* (2nd ed.). Wiley. [Crossref]